

A novel dynamic step size LMS optimization scheme for interference reducing in FBMC-QAM^①

DONG Qiyang(董琪阳)^②, MA Tianming^②, JIANG Xiaoxiao, MA Honglei

(School of Electrical and Electronic Engineering, Shanghai University of Engineering Science, Shanghai 201620, P. R. China)

Abstract

Filter bank multicarrier quadrature amplitude modulation (FBMC-QAM) will encounter interference and noise during the process of channel transmission. In order to suppress the interference in the communication system, channel equalization is carried out at the receiver. Given that the conventional least mean square (LMS) equilibrium algorithm usually suffer from drawbacks such as the inability to converge quickly in large step sizes and poor stability in small step sizes when searching for optimal weights, in this paper, a design scheme for adaptive equalization with dynamic step size LMS optimization is proposed, which can further improve the convergence and error stability of the algorithm by calling the Sigmoid function and introducing three new parameters to control the range of step size values, adjust the steepness of step size, and reduce steady-state errors in small step stages. Theoretical analysis and simulation results demonstrate that compared with the conventional LMS algorithm and the neural network-based residual deep neural network (Res-DNN) algorithm, the adopted dynamic step size LMS optimization scheme can not only obtain faster convergence speed, but also get smaller error values in the signal recovery process, thereby achieving better bit error rate (BER) performance.

Key words: filter bank multicarrier quadrature amplitude modulation (FBMC-QAM), adaptive equalization, least mean square (LMS), dynamic step size

0 Introduction

The 4th-generation mobile communication technology (4G) adopts orthogonal frequency division multiplexing (OFDM) technology, which requires the subcarriers to be strictly orthogonal to reduce inter-carrier interference (ICI)^[1]. Unfortunately, cyclic prefix (CP) in OFDM consumes a certain amount of spectrum resources. In order to improve spectrum utilization, many scholars have focused on new multi-carrier modulation technologies based on OFDM, a good case in point is filter bank multicarrier (FBMC) modulation^[2]. FBMC is composed of an analysis filter bank (AFB) and a synthesis filter bank (SFB), which does not require strict orthogonality between subcarriers. Meanwhile, unlike the rectangular window filter adopted in OFDM, the prototype filter applied in FBMC can not only greatly reduce the out-of-band emissions (OOBE), but also further improve spectral efficiency

by eliminating CP^[3].

Conventional FBMC system adopts offset quadrature amplitude modulation (OQAM). OQAM transmits the imaginary and real parts of the data signal separately, which differ by one-half unit time, transmit the imaginary symbol when the interference is a real number and transmit the real number symbol when the interference is an imaginary number^[4]. In essence, this modulation method does not solve the interference of the imaginary part, and because of the poor compatibility between OQAM and multiple-input multiple-output (MIMO) technology, the resources of the already mature OFDM are wasted^[5]. The quadrature amplitude modulation (QAM) in OFDM not only transmits real and imaginary signals at the same time but also improves transmission efficiency and can be well integrated with existing MIMO. Compared with the OFDM system used in 4G, FBMC-QAM can be better compatible with existing hardware devices, the difference is that the filter used in OFDM is rectangular which requires CP, while

① Supported by the National Natural Science Foundation of China (No. 61601296, 61701295), the Science and Technology Innovation Action Plan Project of Shanghai Science and Technology Commission (No. 20511103500) and the Talent Program of Shanghai University of Engineering Science (No. 2018RC43).

② To whom correspondence should be addressed. E-mail: tmma@sues.edu.cn.
Received on Jan. 23, 2024

FBMC-QAM applies a prototype filter without CP^[6].

Like OFDM, FBMC-QAM will also encounter interference in the process of channel transmission, and when the signal is transmitted to the receiver, the quality of the signal will deteriorate. In order to suppress the interference, it is necessary to add an equalizer at the receiver to eliminate the influence of the channel, and the signal that arrives at the receiver after transmission through the channel is processed contrary to the channel characteristics, and finally the received signal is recovered as correctly as possible. Generally, equalizers can be divided into two categories: linear equalization and nonlinear equalization. Linear equalization mainly includes the zero forcing (ZF) algorithm^[7] and the minimum mean square error (MMSE) algorithm^[8], while nonlinear equalization applies the decision result as feedback to further adjust the equalizer when determining the signal output value. A good case in point is the least mean square (LMS) algorithm.

Ref. [9] adopted the conventional fixed step LMS algorithm to divide the received signal into the expected signal and the auxiliary signal, and iteratively solves the weight parameters through an adaptive structure to make the weighted auxiliary signal close to the target signal, thereby forming a spatial spectral peak in the direction of signal arrival. Ref. [10] proposed a novel residual network-based approach called Res-DNN that utilizes deep learning to replace conventional channel equalization and demapping modules. Unfortunately, the algorithms in Ref. [9] and Ref. [10] have the drawback of slow convergence speed.

In this paper, the conventional LMS is improved by calling the Sigmoid function and adding new parameters to transform the conventional fixed step size into a dynamic step size. Meanwhile, a dynamic step size LMS optimization adaptive scheme is proposed, which not only achieves faster convergence speed but also further improves the signal error value and enhances the performance of the system.

1 FBMC-QAM system model

The transmitter system architecture of FBMC-QAM can be shown in Fig. 1^[11]. The transmitter outputs a discrete frequency-domain sequence group $\mathbf{X}_{m,n}$, which can be expressed as Eq. (1).

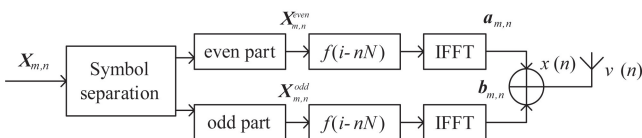


Fig. 1 The architecture of a FBMC-QAM transmitter system

$$\mathbf{X}_{m,n} = [X_{0,n}, X_{1,n}, \dots, X_{N-1,n}]^T \quad (1)$$

where, $0 \leq m \leq N-1$ is the number of subcarriers in the frequency-domain and $n \in \{0, 1, \dots, N-1\}$ is the number of sequences in the time-domain.

By performing odd and even sampling on $\mathbf{X}_{m,n}$ separately, two sequence groups $\mathbf{X}_{m,n}^{\text{even}}$ and $\mathbf{X}_{m,n}^{\text{odd}}$ with $N/2$ frequency-domain sequences can be obtained, which can be represented as

$$\mathbf{X}_{m,n}^{\text{even}} = [X_{0,n}, X_{2,n}, \dots, X_{2t,n}]^T \quad (2)$$

$$\mathbf{X}_{m,n}^{\text{odd}} = [X_{1,n}, X_{3,n}, \dots, X_{2t+1,n}]^T \quad (3)$$

where $t \in \{0, 1, \dots, N/2-1\}$.

$\mathbf{X}_{m,n}^{\text{even}}$ and $\mathbf{X}_{m,n}^{\text{odd}}$ are respectively multiplied by the prototype filter $f(i-nN)$ and performed by inverse fast Fourier transform (IFFT) operation to obtain two time-domain sequences $\mathbf{a}_{m,n}$ and $\mathbf{b}_{m,n}$, which can be formulated as

$$\begin{aligned} \mathbf{a}_{m,n} &= F^{-1} \{ \mathbf{X}_{m,n}^{\text{even}} f(i-nN) \} \\ &= \sum_{t=0}^{2t} \mathbf{X}_{m,n}^{\text{even}} f(i-nN) e^{j2\pi it/N} \end{aligned} \quad (4)$$

$$\begin{aligned} \mathbf{b}_{m,n} &= F^{-1} \{ \mathbf{X}_{m,n}^{\text{odd}} f(i-nN) \} \\ &= \sum_{t=0}^{2t-1} \mathbf{X}_{m,n}^{\text{odd}} f(i-nN) e^{j2\pi it/N} \end{aligned} \quad (5)$$

where $F^{-1} \{ \cdot \}$ represents IFFT operation and i is the time-index of the prototype filter $f(i-nN)$.

The output signal of the transmitter $x(n)$ can be denoted as

$$x(n) = \sum_{n \in Z} \mathbf{a}_{m,n} + \mathbf{b}_{m,n} \quad (6)$$

where Z represents the set of integers.

$x(n)$ arrives at the receiver after transmission through the wireless channel and the signal $y(n)$ at the receiver can be demonstrated by

$$y(n) = h(n) * x(n) + v(n) \quad (7)$$

where, $h(n)$ is the impulse response of the channel, $v(n)$ is the additive white Gaussian noise (AWGN) in the channel, and $*$ is convolutional operations.

The signal of a single carrier exists in the time domain, whereas for multicarrier modulation, it is transformed from the time domain to the frequency domain after undergoing a Fourier transform through the filter, which is also known as Eqs (4) – (5). In order to simplify the expression of the unification equation, so for the representation of $\mathbf{X}_{m,n}$ the frequency domain representation is used.

2 Equalizer model

After reaching the receiver, it goes through an equalizer for channel equalization. The time domain

symbols of the transmitter have been given at the sending end, and for the generated time series, the odd and even numbers are processed separately, and each of them is processed by the filter and summed up together, which is the working process of Eqs (4) – (6) to get $x(n)$. $x(n)$ is added to the noise channel of $v(n)$ to get $y(n)$ after the impulse response of the channel of $h(n)$. Eqs (1) – (6) are the working process of the transmitter channel before transmitter signal enters into the equalizer. The transmitter time-domain symbols received by the receiver are essentially a transformation of the generated sequence, because the generated sequence is known and can be used directly by the receiver here. Fig. 2 shows the schematic diagram of the adaptive filter^[12], where the receiving signal $y(n)$ is the input signal of the adaptive filter and $s(n)$ is the output of the adaptive filter, which can be depicted as $s(n) = w(n) * y(n)$

$$= w(n) * h(n) * x(n) + w(n) * v(n) \quad (8)$$

where, $*$ represents convolution operation and $w(n)$ denotes equalizer coefficients.

Since $w(n) * h(n)$ is equal to the unit impulse function $\delta(n)$, the signal estimate $s(n)$ at the output of the equalizer can be represented as

$$s(n) = x(n) + w(n) * v(n) \quad (9)$$

Thus, it is not difficult to discover that in order to make $s(n)$ as close as possible to $x(n)$, the equalizer needs to eliminate the influence of $v(n)$ as much as possible.

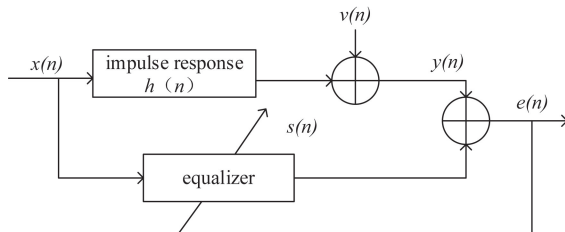


Fig. 2 The schematic diagram of an adaptive filter

Assume the length of the equalizer is N , its input signal $\mathbf{X}_N(n)$ and weight vector $\mathbf{W}_N(n)$ at time n can be respectively formulated as

$$\mathbf{X}_N(n) = [x_0(n), x_1(n), \dots, x_{n-1}(n)]^T \quad (10)$$

$$\mathbf{W}_N(n) = [w_0(n), w_1(n), \dots, w_{n-1}(n)] \quad (11)$$

The output vector at the output of the equalizer can be expressed as

$$\mathbf{s}(n) = \mathbf{W}_N^T(n) \mathbf{X}_N(n) \quad (12)$$

The error relation between the equalizer output signal and the desired signal $\mathbf{d}(n)$ can be represented as

$$\begin{aligned} \mathbf{e}(n) &= \mathbf{d}(n) - \mathbf{s}(n) \\ &= \mathbf{d}(n) - \mathbf{W}_N^T(n) \mathbf{X}_N(n) \end{aligned} \quad (13)$$

The cost function of the adaptive filter can be de-

fined by $J(n) = E[e^2(n)]$, which E represents the mean square of the error value, $e(n)$ represents error relation between the equalizer output signal and the desired signal. Obviously, $J(n)$ should be as small as possible, which is determined by $\mathbf{W}_N(n)$. In order to obtain the optimal solution, the idea of minimum gradient is applied to update $\mathbf{W}_N(n)$ for each iteration, which can be formulated as

$$\begin{aligned} \mathbf{W}_N(n+1) &= \mathbf{W}_N(n) - \mu \nabla[J(n)] \\ &= \mathbf{W}_N(n) - \mu \nabla\{E[e^2(n)]\} \end{aligned} \quad (14)$$

where μ is the step size parameter in the algorithm that is updated along the descending direction and $\nabla[J(n)]$ represents taking the gradient of $J(n)$, which can be formulated as

$$\begin{aligned} \nabla[J(n)] &= \frac{\partial\{E[e^2(n)]\}}{\partial \mathbf{W}_N} \\ &= 2E\left[e(n) \frac{\partial e(n)}{\partial \mathbf{W}_N}\right] \\ &= 2E[e(n) \cdot (-\mathbf{X}_N(n))] \\ &= -2e(n) \mathbf{X}_N(n) \end{aligned} \quad (15)$$

Thus, the weight formula for the equalizer of the LMS can be re-expressed as

$$\mathbf{W}_N(n+1) = \mathbf{W}_N(n) + 2\mu e(n) \mathbf{X}_N(n) \quad (16)$$

3 Dynamic step size algorithm

The weights of the equalizer are related to the step size parameter μ . The larger μ , the fewer iterations, and the more rapid the entire convergence process. For the equalization system, if the step size μ can be dynamically controlled, the equalization error $e(n)$ can be minimized. In the equilibrium starting stage, $e(n)$ is larger, as the error gradually becomes smaller with continuous iteration, the step size also needs to be casually smaller. Therefore, the Sigmoid function is applied, which can be formulated as^[13]

$$\text{Sig}(n) = 1 - e^{-1} \quad (17)$$

Since the Sigmoid function is a function with strict monotonicity, therefore, it can be utilized to change the static step size μ becomes the dynamic step size $\mu(n)$, which can be expressed as

$$\mu(n) = \gamma(1 - e^{-\omega |e(n)|^p}) \quad (18)$$

where, γ ($0 < \gamma < 1$) is applied to control the range of values of the step size, ω is used to regulate the trend of the values of the step size and control the monotonicity of the system. ω is related to the initial value of the input, which is usually less than 0.5 to accelerate convergence. Since the coefficient ω can completely control the direction of the step function $\mu(n)$, under the condition of guaranteeing γ , ω is turned into a function related to $e(n)$, and a control factor c is added. c is a

variable close to 1, it fluctuates slightly up and down as compensation for the error, which can be represented as

$$\omega(n) = c |e(n)e(n-1)| \quad (19)$$

The above equation associates the coefficient ω with the equilibrium error $e(n)$, and with the help of the equilibrium error $e(n-1)$ of adjacent moments as a feedback reference^[14], the correlation function of the two realizes that when the error is small, the coefficient ω becomes smaller, so as to achieve the role of controlling the step-size, and the variable step-size function can be expressed as

$$\mu(n) = \gamma(1 - e^{-c |e(n)e(n-1)| \cdot |e(n)|^2}) \quad (20)$$

Therefore, it can be seen from the above that not only can the weights of the equalizer be changed in real-time by means of gradient descent to better achieve the minimal value required by the cost function, but also through the relationship between the dynamic step size as well as the control factor, the step size is changed from the original uncontrollable to controllable and converges faster in the stage of a large step by the characteristic that the product of the equalization errors of the neighboring equilibrium becomes smaller, and it can be kept relatively stable in the stage of a small step. Thus, the stability of the output signal is guaranteed.

The specific implementation steps of the proposed dynamic step LMS algorithm are as follows, and its flowchart is shown in Fig. 3.

Step S1 For each input $x(n)$, compute the output signal $s(n)$;

Step S2 Initialize $W(0)$, $x(0)$;

Step S3 Using the desired output $d(n)$, compute the error signal $e(n)$ to obtain the gradient ∇ ;

Step S4 γ is applied to control the step length range, the specific size can be adjusted according to the initial $e(0)$. During large step length stage, adjust the coefficient ω , as small as possible can achieve the effect of rapid convergence; in the step length of a relatively small stage, for the coefficient ω for a small amount of adjustment, according to the obtained $e(n)$ to determine whether it is necessary to end for the coefficient ω of adjustment;

Step S5 Return to step S2 until the end to obtain the output sequence and the error sequence.

4 Performance simulation and result analysis

For a given FBMC-QAM system, the simulation parameters are shown in Table 1. In view of the time-varying characteristics in real 5G mobile communication channels, International Telecommunication Union Vehicle Channel B (ITU-VB)^[15] is chosen as the wireless channel model for system simulation.

Fig. 4 (a) and (b) show the input raw signal and the waveforms obtained after passing through the noisy channel, the recovered signals are compared by comparing the conventional LMS, the Res-DNN model used in the Ref. [10] and the dynamic LMS proposed in this paper for denoising the noisy signals, respectively.

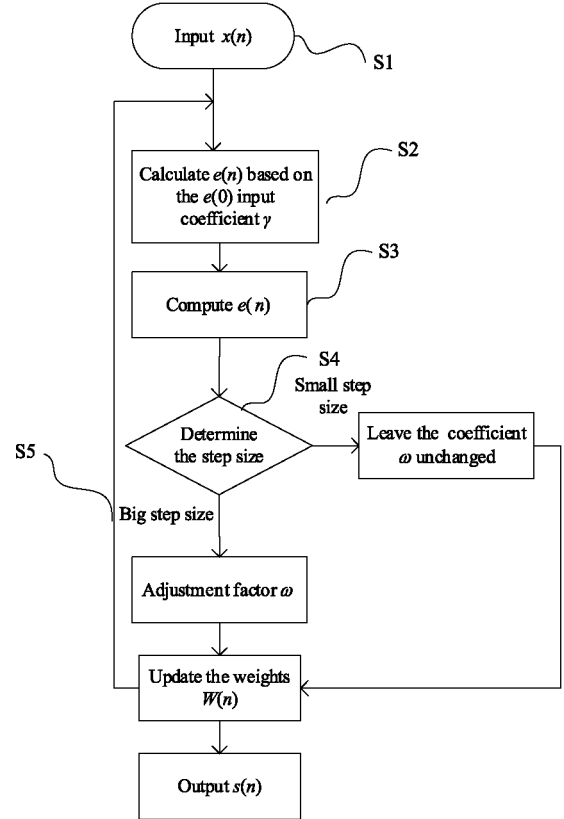


Fig. 3 The flowchart of proposed dynamic step LMS algorithm

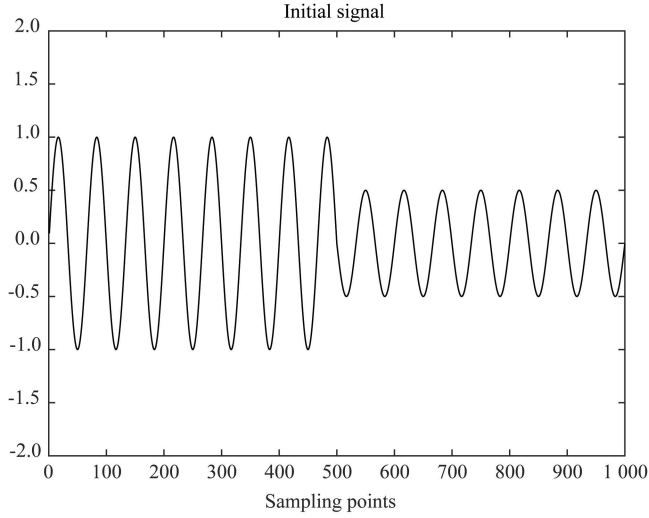
Table 1 System simulation parameters

Parameter name	Parameter value
Modulation method	4QAM
Number of subcarriers (M)	1 024
Overlap factor (K)	4
Number of sampling points	1 000
Number of iterations	100
Equalizer model	LMS, Res-DNN
Channel model	dynamic LMS
Noise model	ITU-VB
	AWGN

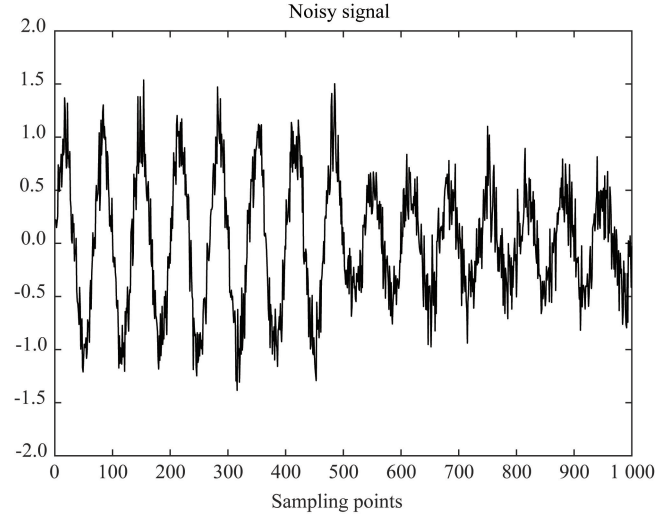
Fig. 5 (a) – (d) illustrate the ideal recovered signal and the waveforms after the noise signal is recovered by three different algorithms, namely, LMS, Res-DNN, and dynamic LMS, respectively. It can be seen that there is less difference between the results of these methods and the ideal signal, because the experiments will be iterated 100 times, and the results of various al-

gorithms are basically not much different after many it-

erations.

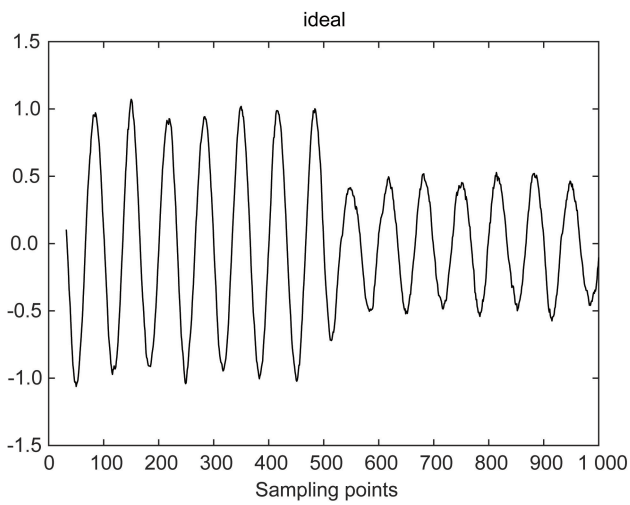


(a) The initial signal at the transmitter

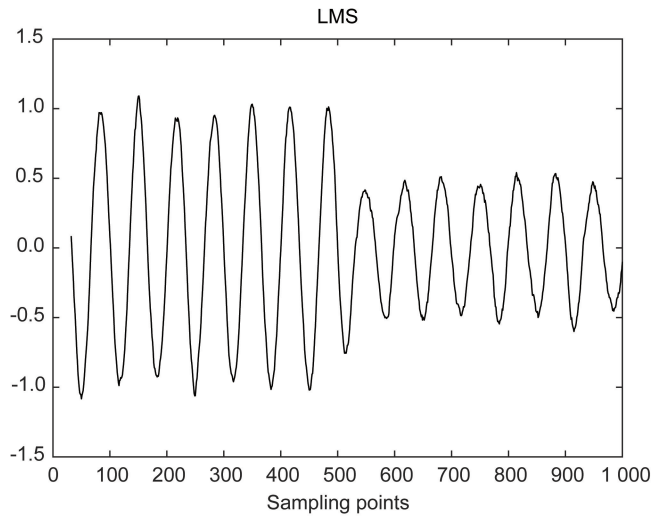


(b) The noisy signal at the receiver

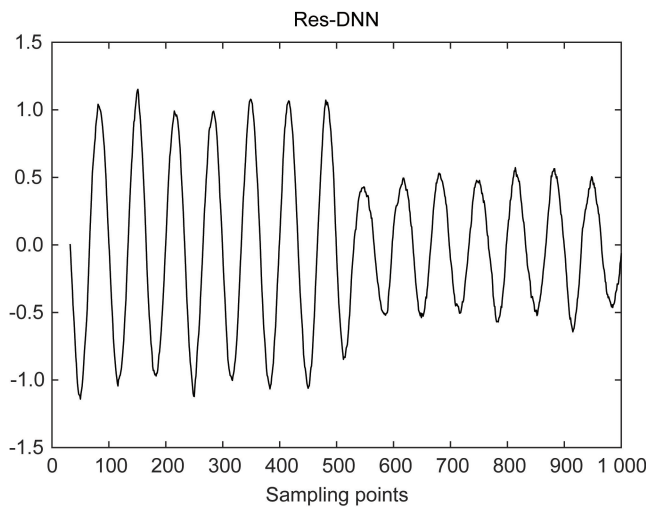
Fig. 4 The signal waveforms



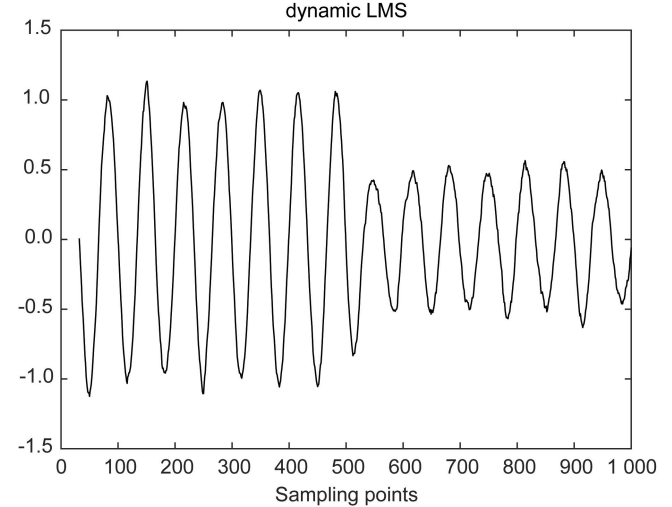
(a) Ideal



(b) LMS



(c) Res-DNN



(d) Dynamic LMS

Fig. 5 The recovered signal by different algorithms

Fig. 6(a) – (d) shows the ideal and errors of the three algorithms in the process of recovering the signal through LMS, Res-DNN, and dynamic LMS, and the errors of the three algorithms in the process of recovering the signal can be clearly seen that for the points after the sampling point of 500, the difference between the al-

gorithms is not so obvious because the weights updated at this time have basically been the same, and the difference between the three algorithms is not so big for the points after the sampling point of 500, that is, in the recovering signal starting stage, the size of the dynamic LMS error is significantly smaller than the other two.

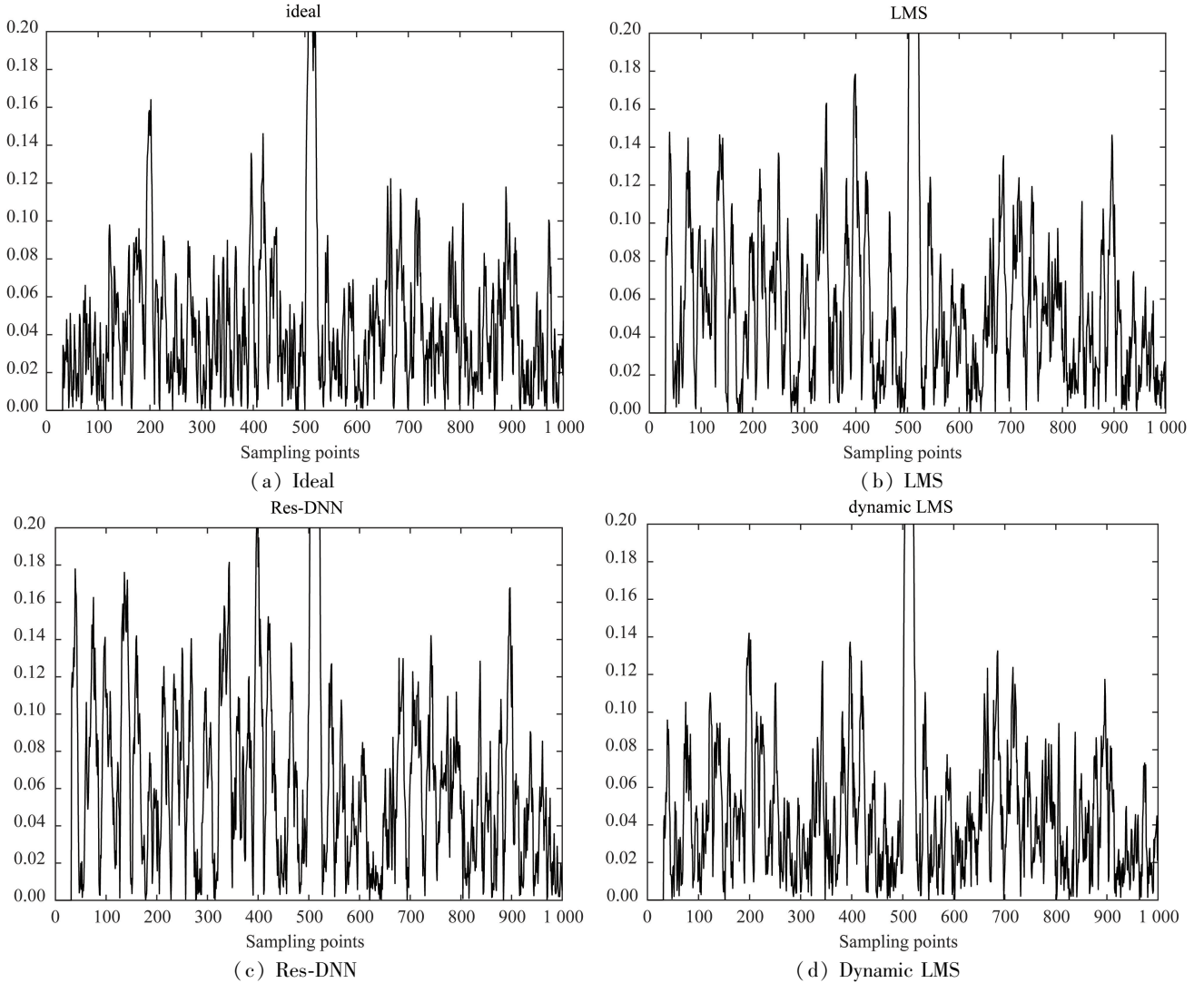


Fig. 6 The error of different algorithms in the recovery process

Fig. 7 is a comparison of the error convergence of the three algorithms and the ideal signal, what can be seen is that the dynamic LMS is very close to the ideal case error $e(n)$, and the convergence speed is much faster than the Res-DNN and the conventional LMS, thanks to the control factors ω and γ , which can be used to adjust the step size in the starting stage, after the initialization of the first weights, to achieve the effect of faster convergence. Res-DNN will be a little slower and the error will be larger because it needs to use the neural network to complete the training in advance, so it will be a little slower and the error will be

larger. Res-DNN converges a little slower and has a larger error because it needs to utilize the neural network to complete the training in advance.

Fig. 8 shows the bit error rate (BER) comparison of the three algorithms with the ideal signal. The BER of conventional LMS is the worst, and dynamic LMS is better than Res-DNN because dynamic LMS not only utilizes the advantages of the conventional LMS, but also can minimize the BER of the system during the whole system recovery process because of the use of the control factor c to use the two neighboring errors $e(n)$ and $e(n-1)$ as a feedback reference.

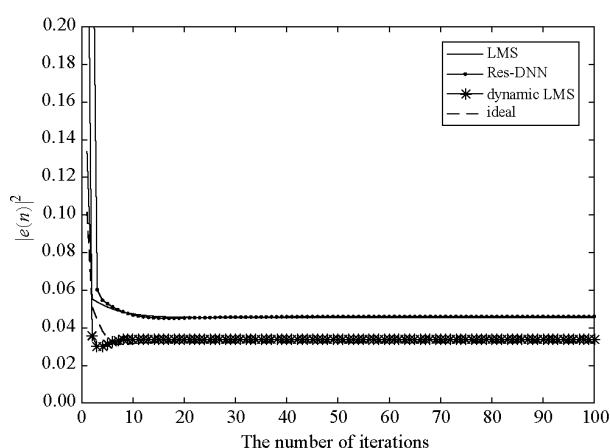


Fig. 7 Convergence comparison of different algorithms

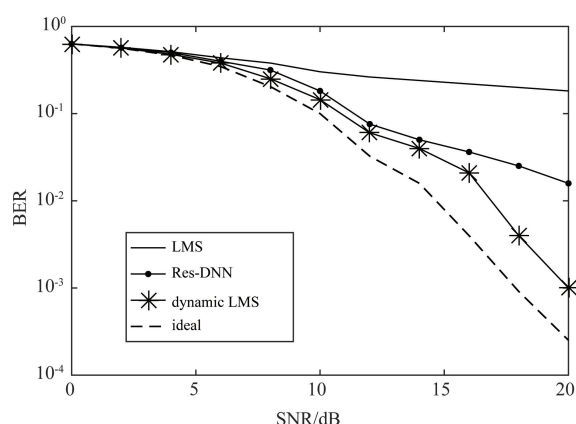


Fig. 8 BER comparison of different algorithms

5 Conclusions

In this paper, a dynamic step size LMS optimization algorithm is proposed based on the conventional fixed-step LMS algorithm. Three kinds of control variables are adopted to control the value of the step size, the steepness, and the steady-state, respectively. The simulation analysis results demonstrate that compared with the conventional LMS algorithm and the neural network-based Res-DNN algorithm, applying the proposed dynamic step size LMS optimization algorithm can achieve a better performance in terms of error size and convergence speed as well as BER.

References

- [1] FARHANG-BOROUEJENY B. OFDM versus filter bank multicarrier [J]. IEEE Signal Processing Magazine, 2011, 28(3): 92-112.
- [2] CHEN D, LAN J, LUO K, et al. Symbol encryption and placement design for OQAM/FBMC systems [J]. IEEE Transactions on Communications, 2022, 70(1): 552-563.
- [3] ANDRADE I G, RUYET D L, CAMPOS M, et al. Bit error probability expressions for QAM-FBMC systems [J]. IEEE Communications Letters, 2022, 26(5): 994-998.
- [4] YOU X, PAN Z, GAO X, et al. 5G mobile communication development trend and some key technologies [J]. China Science: Information Science, 2014, 44(5): 551-563.
- [5] GUPTA A, JHA R K. A survey of 5G network: architecture and emerging technologies [J]. IEEE Access, 2014, 3: 1206-1232.
- [6] NAM H, CHOI M, HAN S, et al. A new filter bank multicarrier system with two prototype filters for QAM symbols transmission and reception [J]. IEEE Transactions on Wireless Communications, 2016, 15(9): 5998-6009.
- [7] BENMEZIANE B, BAUDAIS J Y, MÉRIC S, et al. Comparison of ZF and MF filters through PSLR and ISLR assessment in automotive OFDM radar [C]// Proceedings of the 18th European Radar Conference. London, UK: EuRAD, 2021: 193-196.
- [8] LIU K, TAO C, LIU L, et al. Asymptotic analysis for low-resolution massive MIMO systems with MMSE receiver [J]. China Communications, 2018, 15(9): 189-199.
- [9] FU X, TENG T, MING W. Efficient DOA estimation algorithm based on unbiased variable-step-size LMS algorithm [C]// Proceedings of the 4th International Conference on Information Communication and Signal Processing. Shanghai, China: ICICSP, 2021: 41-44.
- [10] CHENG X, LIU D, ZHU Z, et al. A ResNet-DNN based channel estimation and equalization scheme in FBMC systems [C]// Proceedings of the 10th International Conference on Wireless Communications and Signal Processing (WCSP). Hangzhou, China: IEEE, 2018: 1-5.
- [11] MAHAMA S, HARBI Y J, BUR A G, et al. Iterative interference cancellation in FBMC-QAM systems [C]// Proceedings of the 2019 IEEE Wireless Communications and Networking Conference. Marrakesh, Morocco: WCNC, 2019: 1-5.
- [12] CHEN X, LIU D, WANG C, et al. Deep learning-based channel estimation and equalization scheme for FBMC systems [J]. IEEE Wireless Communications Letters, 2019, 8(3): 881-884.
- [13] ELEKES M, NAGY A, SÁNDOR D, et al. A graphBLAS solution to the SIGMOD 2014 programming contest using multi-source BFS [C]// Proceedings of the 2020 IEEE High Performance Extreme Computing Conference (HPEC). Waltham, USA: IEEE, 2020: 1-7.
- [14] CHEN Z, WANG Z. LMS step size optimization based on Adagrad algorithm [J]. Electronic Production, 2023, 31(14): 83-86.
- [15] Rec. ITU-R M. 1225. Guidelines for evaluation of radio transmission technologies for IMT-2000. Question ITU-R 39/8 [S]. 1997.

DONG Qiyang, born in 1998. He is an M. S. candidate at Shanghai University of Engineering Science. He received his B. S. degree from China Mining University in 2020. His research interests include FBMC communication technology and interference reduction technology.